Field Evaluations on a Prototype System of Cooperative Multi-Cell MIMO Transmission for Asynchronous Inter-Site Base Station Networks

Manabu Mikami†, Masayuki Miyashita, Haruya Miyajima, Kenji Hoshino, Hitoshi Yoshino, and Teruya Fujii
Wireless System R&D Center, Softbank Mobile Corp.
2-5-10 Aomi, Koto-ku, Tokyo, 135-8070 Japan
†E-mail: manabu.mikami@g.softbank.co.jp

***Abstract*—For next generation cellular mobile communication systems, cooperative multi-cell MIMO transmission (cooperative MIMO) technologies, in which multiple base stations (BSs) coordinate their wireless transmission, have recently been receiving considerable attention due to their potential cell-boundary throughput improvement. However, there are few studies that provide field evaluation of cooperative MIMO in real radio-propagation environments. To evaluate cooperative MIMO in a real field, BSs located at different sites should be synchronized to each other with high accuracy in asynchronous inter-site BS networks. We develop a prototype of an experimental system by using a GPS (Global Positioning System)-based inter-BS synchronous controller. We conduct field experiments on two cooperative MIMO transmission schemes: (i) cooperative MIMO-SDM based on space division multiplexing and (ii) Cooperative MIMO-SFBC based on space frequency block coding. We confirm that cooperative MIMO technologies improve the cell-boundary throughput in real radio-propagation environments. This paper describes the developed field experimental system and its field evaluation results. It also shows the effectiveness of cooperative MIMO wireless transmission at the cell-boundary.**

Keywords; cooperative multi-cell MIMO wireless transmission, field experiment, cell-boundary throughput, asynchronous inter-site base station network

I. INTRODUCTION

In next generation cellular mobile communication systems, such as IMT-Advanced or LTE-Advanced, it is required to improve cell-boundary throughput and cell throughput as well as peak throughput [1],[2]. Cooperative multi-cell MIMO transmission (cooperative MIMO) technologies, in which multiple base stations (BSs) are synchronized to each other and coordinate their wireless transmission, are receiving considerable attention due to their potential in improving cell-boundary throughput [3],[4]. In cooperative MIMO, the radio propagation channels between the transmit antennas at coordinated base stations and the receive antennas at a cell-boundary mobile station are regarded as a virtual MIMO (Multiple Input Multiple Output) channel. This channel offers improved channel capacity at the cell-boundary.

Most of previous works on cooperative MIMO evaluate the wireless transmission performances by computer simulations. Few studies have attempted field evaluations in real radio-propagation environments. In order to conduct field evaluations, we have developed a prototype of an experimental system, and confirmed its basic radio transmission performance in laboratory experiments with a fading simulator [5]. For implementing cooperative MIMO in asynchronous inter-site BS networks, high-accuracy inter-BS synchronization is an essential requirement [6]. Our field experimental system synchronizes multiple base stations located at different sites each other with high accuracy by using a GPS based inter-BS synchronization controller. We conduct field experiments on two cooperative MIMO transmission schemes: (i) cooperative MIMO-SDM based on space division multiplexing over BS antennas located at different sites and (ii) cooperative MIMO-SFBC based on transmit diversity with space frequency block coding over the non co-sited BS antennas. This paper describes the developed field experimental system and its field evaluation results in an asynchronous inter-site base station network. It also shows the effectiveness of cooperative MIMO wireless transmission at the cell-boundary in a real radio-propagation environment.

II. FIELD EXPERIMENTAL SYSTEM

A. System Configuration

Figure 1 illustrates the network configuration of our field experimental system. Table I summarizes the key specifications of wireless transmission. The system is composed of two experimental base stations (BSs), each equipped with a transmit antenna, and an experimental mobile station (MS) equipped with two receive antennas. Note that BS #1 and BS #2 are located at different sites. With regard to the antenna configuration, the radio propagation channel between the BS transmit antennas and the MS receive antennas can be regarded as a virtual 2x2 MIMO channel. In the field experimental system, the non co-sited BSs, BS #1 and BS #2, transmit orthogonal frequency division multiplexing (OFDM) signals with the center frequency of 3.3 GHz, the sub-carrier spacing of 15 kHz, the sub-frame lengths of 1 ms and the frame lengths of 10 ms. In each BS transmitter, the OFDM signals are generated after modulated data symbols are multiplexed with preamble symbols for timing detection and with reference symbols for channel

This work was partially sponsored by the Ministry of Internal Affairs and Communications of Japan, under the grant, "R&D on the cooperative control technologies for multiple base stations in an environment consisting of various cell sizes".

978-1-4673-0990-5/12/$31.00 ©2012 IEEE

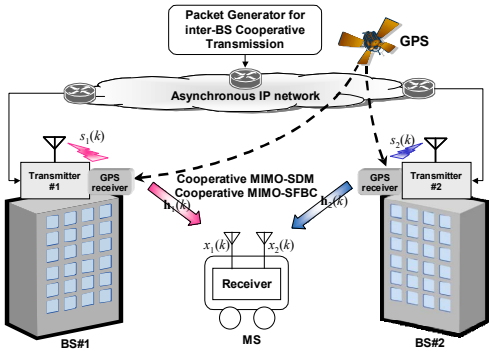

Figure 1. Network configuration of the field experimental system.

TABLE I. KEY SPECIFICATIONS OF WIRELESS TRANSMISSION

Number of BSs/MSs	BS: 2 / MS: 1
Number of antennas	TX side : 1 (per BS) /RX side: 2 (MS)
Radio frequency	3.3 GHz band
OFDM parameters	Number of assigned data sub-carriers: 72, Sub-carrier spacing: 15kHz, Guard Interval (GI) duration: 16.67 μs
Subframe lengths	1 ms (12 OFDM symbols)
Frame lenghs	10 ms (1 preamble subframe + 9 data subframes)
Preamble symbols	PSK modulated Zadoff-Chu sequence
Reference symbols	QPSK modulated truncated Gold sequence
Data modulation	QPSK, 16QAM, 64QAM
Channel coding	Turbo coding (Constraint lengths : 4, Embedded interleaver : Prime interleaver, Coding rate R = 1/3)
Cooperative MIMO transmission scheme	Cooperative MIMO-SDM, Cooperative MIMO-SFBC
FFT timing detection	Peak search of sliding correlation between received signal and replica of preamble symbols
Channel estimation	Reference-symbol assisted channel estimation based on IFFT/FFT interpolation with sinc-function channel replica [7]
Signal detection	Cooperative MIMO-SDM: MMSE Cooperative MIMO-SFBC: MRC
Channel decoding	Max Log-MAP decoding (8 iterations)
Block error detection	24 bit cyclic redundancy check (CRC)

estimation at the MS receiver, respectively. In the field experimental system, the two cooperative MIMO transmission schemes, cooperative MIMO-SDM and cooperative MIMO-SFBC, were implemented. At each BS transmitter, user data sequences are channel-coded by a turbo-code with coding rate of 1/3. At the MS receiver, the received signals are channel-decoded by the Max Log-MAP algorithm with eight iterations.

Figures 2 and 3 illustrate the radio frame/subframe format and the resource assignment of reference symbols, respectively. As shown in these figures, the preamble symbols are allocated at the first subframe in each radio frame and the reference symbols are orthogonal to the modulate data symbols in both the time-domain and the frequency-domain so as to keep high channel estimation accuracy. Figures 4 (a) and (b) provide block diagrams of the BS transmitter and MS receiver, respectively. As shown in Fig. 4 (a), the coordinated BSs are synchronized to each other with high accuracy by using a GPS based inter-BS synchronous controller [6] that prevents the timing offset between the received signals of BS

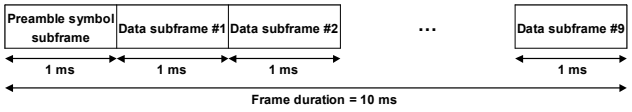

Figure 2. Radio frame/subframe format.

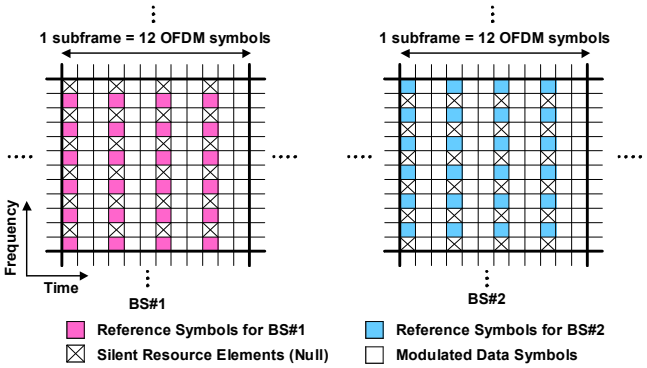

Figure 3. Resource element mapping to reference symbols in data subframes

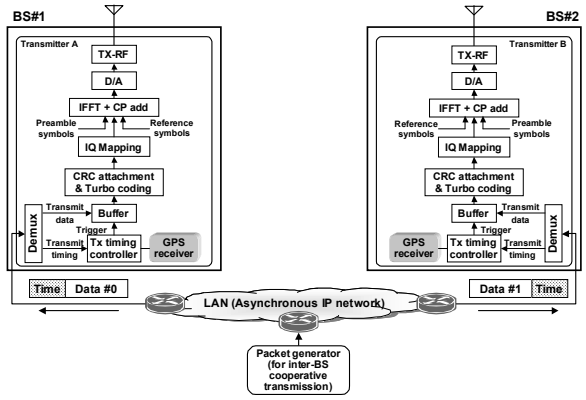

(a) BS transmitters

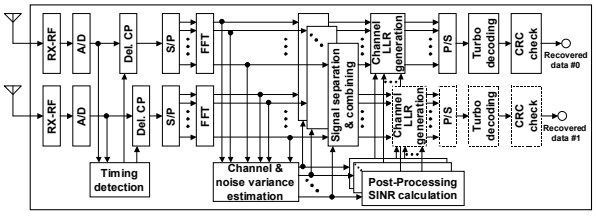

(b) MS receiver

Figure 4. Block diagrams of wireless transmission equipment.

#1 and BS #2 from exceeding the Guard Interval (GI) duration of OFDM signals. The synchronization control establishes inter-BS synchronization even though the base stations are connected to each other via asynchronous IP (Internet Protocol)-based inter-site BS networks. As shown in Fig. 4 (b), in the MS receiver, the optimal position of the Fast Fourier Transform (FFT) window is detected from the received signal. The virtual 2x2 MIMO channel is estimated from the received reference symbols by using FFT-based interpolation algorithm [7]. By using the channel estimation result, the desired signal sequences are detected based on the received signal processing described in the next subsection.

B. Received Signal Processing at MS receiver

This subsection presents the received signal processing at the MS receiver. It first describes the received signal representation, and then it describes the soft-reliability information calculation for turbo decoding.

1) Received Signal Representation

As shown in Fig.1, let $\mathbf{h}_j(k)$ be the frequency channel response for the k-th subcarrier between the j-th BS antenna ($j=1,2$ corresponds to BS #1 and BS #2, respectively) and the MS antennas, the received signal vector at MS, $\mathbf{x}(k)$ can be expressed as

$$\mathbf{x}(k)=\mathbf{H}(k)\mathbf{s}(k)+\mathbf{n}(k), \quad (1)$$

$$\mathbf{H}(k)=[\mathbf{h}_1(k)\ \ \mathbf{h}_2(k)], \quad (2)$$

$$\mathbf{s}(k)=[s_1(k)\ \ s_2(k)]^T,\ s_j(k)\in\{s_{\text{rep}}^{(m)}\}\ (m=1,\cdots,M_{ary}), \quad (3)$$

$$E\{|\,s_j(k)\,|^2\}=1, \quad (4)$$

where $s_j(k)$, $\mathbf{n}(k)$, M_{ary}, $s_{\text{rep}}^{(m)}$, and $E\{\cdot\}$ denote the transmitted signal of j-th BS, the receiver noise vector, the modulation order, the m-th candidate of the transmitted complex symbol value, and ensemble average, respectively.

2) Soft Reliability Information Calculation

a) Cooperative MIMO-SDM

In cooperative MIMO-SDM, the desired signal sequences are spatially demultiplexed based on minimum mean square error (MMSE) filtering with the channel estimation result at the MS receiver. The output signal of the MMSE filter of the j-th sub-stream, $y_j(k)$, can be expressed as

$$y_j(k)=\mathbf{w}_j^H(k)\mathbf{x}(k), \quad (5)$$

$$\mathbf{w}_j(k)=\{\mathbf{H}^H(k)\mathbf{H}(k)+P_N\mathbf{I}\}^{-1}\mathbf{h}_j(k), \quad (6)$$

where $\mathbf{w}_j(k)$, $\{\cdot\}^H$, P_N, and $\mathbf{I}$ represent the MMSE filter coefficient vector, the conjugate transpose, the average noise density of each receive antenna, and the unit matrix, respectively. The post-processing SINR at the output of the MMSE filter of the j-th sub-stream, $\text{SINR}_{\text{out},j}(k)$, is calculated by [8]

$$\text{SINR}_{\text{out},j}(k)=\frac{\mathbf{w}_j^H(k)\mathbf{h}_j(k)}{1-\mathbf{w}_j^H(k)\mathbf{h}_j(k)}, \quad (7)$$

Note that soft-decision channel decoders such as turbo decoders require soft-reliability information such as channel LLR (Log-Likelihood Ratio) of each transmitted bit. Let $c_j(k,l)\in\{0,1\}$ and $c_{\text{rep}}^{(m)}(l)\in\{0,1\}$ denote the l-th logical bit values of $s_m(k)$ and $s_{\text{rep}}^{(m)}$, respectively. The channel LLR of each transmitted bit, $L_{ch}(c_j(k,l))$, is calculated as follows [8]

$$L_{ch}(c_j(k,l))=\text{SINR}_{\text{out},j}(k)\left\{\min_{m\in\{s_{\text{rep}}^{(m)}|c_{\text{rep}}^{(m)}(l)=1\}}|\,y_j(k)-s_{\text{rep}}^{(m)}\,|^2-\min_{m\in\{s_{\text{rep}}^{(m)}|c_{\text{rep}}^{(m)}(l)=0\}}|\,y_j(k)-s_{\text{rep}}^{(m)}\,|^2\right\}. \quad (8)$$

b) Cooperative MIMO-SFBC

In cooperative MIMO-SFBC is employed, the same data sequence is transmitted from both BS #1 and BS #2, The transmitted signal sequence $s(k)$ $(k=2i,2i+1)$ is pre-coded by Alamoti's code and the transmitted signal vector, $\mathbf{s}(k)$ $(k=2i,2i+1)$, can be expressed as [9]

$$\mathbf{s}(2i)=\begin{bmatrix}s(2i)\\ s(2i+1)\end{bmatrix},\ \mathbf{s}(2i+1)=\begin{bmatrix}-s^*(2i+1)\\ s^*(2i)\end{bmatrix}. \quad (9)$$

where $\{\cdot\}^*$ denotes the conjugate. From eqs (1), (2), and (9), the following matrix equation is obtained

$$\begin{bmatrix}\mathbf{x}(2i)\\ \mathbf{x}^*(2i+1)\end{bmatrix}=\begin{bmatrix}\mathbf{H}(2i)\\ \mathbf{H}^*(2i+1)\mathbf{P}\end{bmatrix}\begin{bmatrix}s(2i)\\ s(2i+1)\end{bmatrix}+\begin{bmatrix}\mathbf{n}(2i)\\ \mathbf{n}^*(2i+1)\end{bmatrix}, \quad (10)$$

where

$$\mathbf{P}=\begin{bmatrix}0 & -1\\ 1 & 0\end{bmatrix}. \quad (11)$$

At the MS receiver, the desired signal sequences are detected based on MRC (Maximum Ratio Combining) with the channel estimation result. Since it is assumed that the difference between adjacent sub-carriers is small enough to be ignored (i.e., $\mathbf{H}(2i+1)\approx\mathbf{H}(2i)$), the output of the MRC signal combiner, $y(k)$ $(k=2i,2i+1)$, can be expressed as

$$\begin{bmatrix}y(2i)\\ y(2i+1)\end{bmatrix}\approx\frac{\mathbf{H}^H(2i)\mathbf{x}(2i)+(\mathbf{H}^*(2i)\mathbf{P})^H\mathbf{x}^*(2i+1)}{\sum_{j=1}^{2}\left\|\mathbf{h}_j(2i)\right\|^2}. \quad (12)$$

The post-processing SINR at the output of the MRC signal combiner, $\text{SINR}_{\text{out}}(k)$, is approximated as

$$\text{SINR}_{\text{out}}(k)\approx\frac{1}{P_N}\sum_{j=1}^{2}\left\|\mathbf{h}_j(k)\right\|^2. \quad (13)$$

As in the case of cooperative MIMO-SDM, the turbo decoder requires soft-reliability information such as channel LLR (Log-Likelihood Ratio) of each transmitted bit. Let $c(k,l)\in\{0,1\}$ denote the l-th logical bit values of $s(k)$. Consequently, the channel LLR value of each transmitted bit, $L_{ch}(c(k,l))$, is calculated as

$$L_{ch}(c(k,l))=\text{SINR}_{\text{out}}(k)\left\{\min_{m\in\{s_{\text{rep}}^{(m)}|c_{\text{rep}}^{(m)}(l)=1\}}|\,y(k)-s_{\text{rep}}^{(m)}\,|^2-\min_{m\in\{s_{\text{rep}}^{(m)}|c_{\text{rep}}^{(m)}(l)=0\}}|\,y(k)-s_{\text{rep}}^{(m)}\,|^2\right\}. \quad (14)$$

III. FIELD EXPERIMENT

A. Experimental Environment

Figure 5 illustrates the experimental site. The area is in a typical suburban area in Chofu-city, Tokyo, Japan. In this experiment, BS #1 and BS #2 were located at buildings separated by about 300m. The BS antennas were mounted on the tops of the buildings with the height of about 30 m above the ground. The MS antennas were mounted on the roof of a van at a height of about 3 m. We first evaluated the BLER (Block Error Rate) performance in a quasi-static environment, i.e., MS was located at the fixed point of "e" in Fig. 5. The radio propagation condition was non-line-of site (NLOS) from both base stations. Then, we also evaluated the throughput performance on the measurement course shown in Fig. 5.

B. Experimental Results in a Quasi-Static Environment

We measured BLER performance of cooperative MIMO-SDM and cooperative MIMO-SFBC at point "e", where signals transmitted from BS #1 and BS #2 were received with almost equal power. We also simultaneously measured delay profiles and spatial fading correlations at point "e".

Figure 6 shows the measured power delay profiles at point "e" by using the reference symbols multiplexed with the modulated data symbols. In this figure, the solid line plots the delay profile between BS#0 transmit antenna and point "e", and the dashed line plots the delay profile between BS#1 transmit antenna and point "e". The measured delay spread between each transmit antenna and each receive antenna was approximately 0.15 μs. The measured fading correlations between each transmit antenna and each receive antenna were almost 0 (uncorrelated). From Fig.6, it is found that the timing offset between the arrived preceding waves transmitted from BS #1 and BS #2 is about 0.30 μs much smaller than the GI of 16.67μs. This result confirms that the field experimental system demonstrates the high-accurate inter-BS synchronization, which is an in dispensable technology for cooperative MIMO in an asynchronous inter-site BS networks.

Figure 7 shows the field experimental results of the BLER performance. In the BLER performance measurement, the transmitted signal was modulated by 16QAM with coding rate of R = 1/3. Instantaneous fading was simulated by moving the van within the short distance of about 3m (corresponds to about 30 wavelengths at the center frequency of the 3.3GHz band). The maximum Doppler frequency was approximately 5 Hz. Figure 7 also shows computer simulation results in which perfect inter-BS synchronization and perfect channel estimation were assumed. In the simulations, the discrete delay path model was generated based on Report ITU-R M.2135 [10] so that the delay spread of the model equals to that of the measurement results, and quasi-static fading uncorrelated between each transmit antenna and each receive antenna was generated.

From Fig.7, it is found that the BLER degradation of the

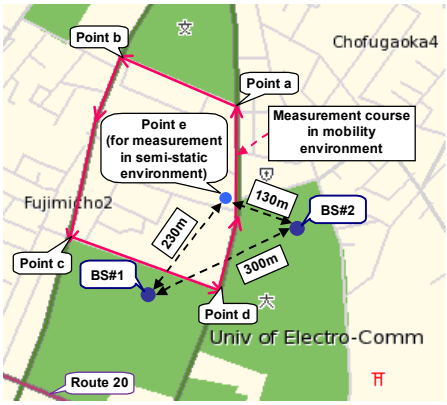

Figure 5. Field experimental site.

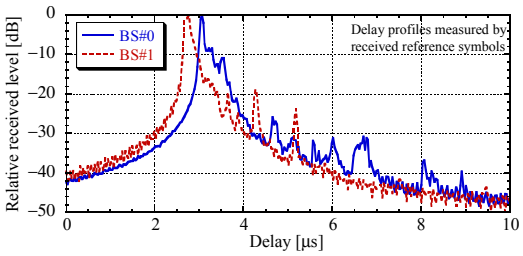

Figure 6. Measured power delay profiles in a semi-static environment.

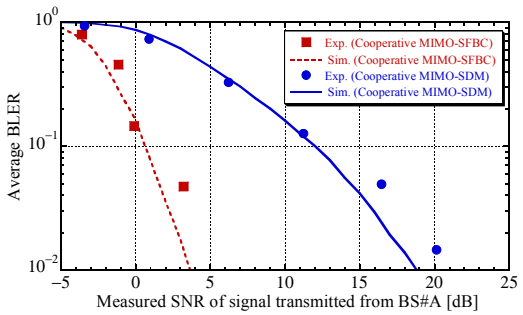

Figure 7. Block error rate performance in a semi-static environment.

field experimental results from the simulation results is less than 2 dB in SNR. The results demonstrate that the field experimental system achieved the intended BLER performance and the implementation of both cooperative MIMO-SDM and cooperative MIMO-SFBC in real radio-propagation environments.

C. Experimental Results in a Mobility Environment

Figure 8 plots examples of normalized throughput and RSRP (Reference Symbol Received Power per sub-carrier) versus running distance along the measurement course. Since the transmitted signals were modulated by 16QAM (= 4 bits/s) with coding rate of R = 1/3 in the experiment, theoretical maximum throughputs are about 2.6 bps/Hz and 1.3 bps/Hz with and without cooperative MIMO-SDM, respectively. The points of "a", "b", "c" and "d" correspond to the corners of the measurement course shown in Fig. 5. The

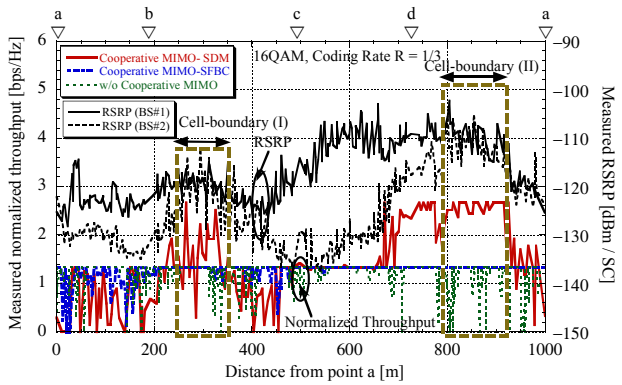

Figure 8. Normalized throughput and RSRP vs. running distance.

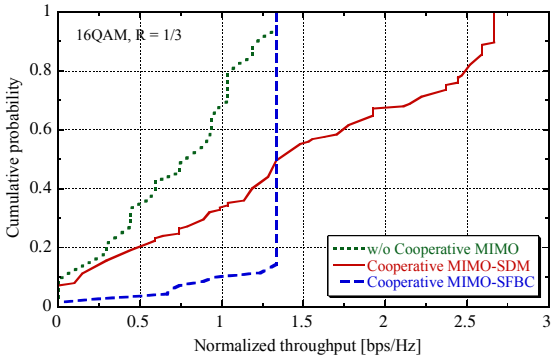

Figure 9. Cumulative probability of cell-boundary throughput.

speed of the van was about 30 km/h. In this experiment, "cell-boundary" is defined as the points where the received signal power of BS #1 is approximately equal to that of BS #2. As shown in Fig. 8, "Cell-boundary (I)" lies between the 250 m point and the 370 m point. "Cell-boundary (II)" lies between the 780 m point and the 930 m point. From Fig. 8, we can conclude that both cooperative MIMO-SDM and cooperative MIMO-SFBC can improve throughputs at the cell-boundary relative to the case of without cooperative MIMO. From Fig. 8, it is also found that the received signal power at cell-boundary (II) is about 10 dB larger than that of cell-boundary (I), and that a high signal-to-noise-power-ratio (SNR) is obtained at cell-boundary (II). Therefore, at cell-boundary (II), both cooperative MIMO-SDM and cooperative MIMO-SFBC almost achieve their theoretical maximum throughputs.

Figure 9 plots the cumulative probability of throughput at cell-boundaries (I) and (II) (data taken from Fig. 8). For comparison, this figure also plots the characteristics of the case without cooperative MIMO in which BS #2 is set as the interfering BS. For example, we evaluate the throughput values at the cumulative probability of 50 % in the case with cooperative MIMO-SDM, with cooperative MIMO-SFBC and without cooperative MIMO. From Fig. 9, it is found that these values are 1.3 bps/Hz, 1.3 bps/Hz and 0.8 bps/Hz, respectively. This result confirms that both cooperative MIMO-SDM and cooperative MIMO-SFBC can improve cell-boundary throughput compared to the case of without cooperative MIMO. Next, we evaluated the throughput values at the cumulative probability of 20 %. From Fig. 9, it is found that cooperative MIMO-SDM improves the throughput value by about 0.8 bps/Hz compared to cooperative MIMO-SFBC. At the cumulative probability of 80 %, Fig. 9 shows that cooperative MIMO-SDM improves the throughput value by about 0.8 bps/Hz compared to cooperative MIMO-SFBC. These results confirm that cooperative MIMO-SDM and cooperative MIMO-SFBC are effective in high and low SNR environments, respectively.

IV. Conclusions

We developed a prototype system for field experimental evaluations of cooperative multi-cell MIMO wireless transmission (cooperative MIMO) technologies and conducted a field experiment on (i) cooperative MIMO-SDM based on space division multiplexing over BS antennas located at different sites and (ii) cooperative MIMO-SFBC based on space frequency block coding over the non co-sited BS antennas, as cooperative MIMO transmission schemes. This paper described the developed field experimental system and showed the field experimental results. We confirmed that cooperative MIMO is very effective in improving the throughput at the cell-boundary.

Acknowledgment

The authors appreciate Mr. Liang Zhang of Softbank Mobile for his assistance in the field experiments.

References

[1] Report ITU-R M.2134, "Requirements related to technical performance for IMT-Advanced radio interface(s)," Dec. 2008.

[2] 3GPP TR36.913, V10.0.0, "Requirements for further advancements for E-UTRA (LTE-Advanced)," March 2011.

[3] H. Zhang and H. Dai, "Cochannel interference mitigation and cooperative processing in downlink multicell multiuser MIMO networks," EURASIP Journal on Wireless Commun. and Networking, vol.2004, no.2 pp.222–235, Feb. 2004.

[4] 3GPP TR36.813, V9.0.0, "Further advancements for E-UTRA physical layer aspects," March 2010.

[5] M. Miyashita, K. Hoshino, M. Mikami, H. Yoshino, and T. Fujii, "A prototype of coordinated multi-BS wireless transmission system," Proc. 2010 IEICE Society Conf., B-5-35, p.389, Sept. 2010.

[6] H. Miyajima, M. Mikami, H. Hayashi, and T. Fujii, "A prototype system for evaluating multi-cell cooperative transmission in asynchronous mobile radio networks," Proc. IEEE VTC2011-Fall, San Francisco, USA, Sept. 2011.

[7] H. Kayama, K. Hiramatsu, and K. Homma, "A study on the accurate channel estimation method applying sinc function based channel replica for a broadband OFDM wireless communication system," IEICE Technical Report, RCS2007-70, Aug. 2007.

[8] D. Seethaler, G. Matz, F. Hlawatsch, "An efficient MMSE-based demodulator for MIMO bit-interleaved coded modulation," Proc. IEEE Globecom2004, pp.2455–2459, Dallas, TX, USA, Nov./Dec. 2004.

[9] G. Li and Y. Gong, "Study on MIMO schemes for 3G-LTE downlink," WSEAS Trans. Commun, vol.8, no.8, pp.883–893, Aug. 2009.

[10] Report ITU-R M.2135, "Guidelines for evaluation of radio interface technologies for IMT-Advanced," Nov. 2008.